Electronic Supplementary Material (ESI) for Green Chemistry.

Supporting information for

Simple Synthesis of self-assembled nacre-like materials with 3D periodic layers from nanochitin *via* hydrogelation and mineralization

Junhua Xu[1,2,‡], Liang Liu[1,‡], Juan Yu[1], Yujun Zou[1], Wenhui Pei[1], Lili Zhang[1], Wenbo Ye[1], Long Bai[2], Zhiguo Wang[1,], Yimin Fan[1,*], Qiang Yong[1], Orlando J. Rojas[2]*

[1]Jiangsu Co-Innovation Center of Efficient Processing and Utilization of Forest Resources, International Innovation Center for Forest Chemicals and Materials, College of Chemical Engineering, College of Light Industry and Food Engineering, Nanjing Forestry University, Nanjing 210037, China.

[2]Bioproducts Institute, Department of Chemical and Biological Engineering, Department of Chemistry and Department of Wood Science, The University of British Columbia Vancouver, BC V6T 1Z3, Canada

‡These authors contributed equally to this work.

*Corresponding avthors: Y. Fan, E-Mail: fanyimin@njfu.edu.cn; Z. Wang, E-Mail: wzg@njfu.edu.cn

Analysis Methods

Titration tests

The degree of deacetylation (DDA) of partially deacetylated chitin and nucleation pH was tested by titration performed with an automatic titrator (HAADDK). The pH of all the solutions was adjusted to 2.5 before titration. Then aqueous alkali solution was added at a 0.1 ml/min rate under constant stir. The pH and electric conductivity were recorded every 30 s, equivalent to 0.05 ml NaOH solution aliquots.

To calculate the DDA of partially deacetylated chitin, 0.1 g were dispersed in 60 ml deionized water and 0.1 M HCl was used to adjust the pH to 2.5. After stirring for 30 min, 0.05 M NaOH was added, and the titration was finished when the pH reached a value of 11.5. The "V" shape titration curve can be draw following the volume of NaOH and conductivity. We drew three tangent lines according to the titration curve, and two intersection points were assigned to the volume of NaOH consumed by the amino groups (ΔV). The DDA can be calculated as follow:

$$DDA = \frac{203 * C * \Delta V}{m + 42 * C * \Delta V}$$

where C is the concentration of NaOH (0.05 mol/L), m is the weight of the partially deacetylated chitin used (0.1 g). To calculate the nucleation pH, several amounts of ion precursor buffer were added in 60 ml deionized water and 0.1 M HCl was used to adjust the pH to 2.5, then 5% wt/v aqueous ammonia was added to the sample. The pH curve was recorded. The concentration of OH^- decreases sharply when nucleation occurs due to formation of HA. The nucleation pH was the turning point in the pH curve.

Transmission electron microscopy (TEM)

TEM images of NCh were acquired using a JEOL JEM-1400 & JEM2100 transmission electron microscope (200 kV). The NCh and LH samples were dispersed in deionized water at a concentration of 0.01% followed by tip ultrasonication to ensure a thorough dispersion. Then the sample was dropped on a copper network covered with carbon film.

X-ray diffraction

XRD data were accessed by using a X-ray diffractometer (Ultima IV) equipped with Cu Kα radiation (λ = 1.54056 Å). The synthetic nacre like HA- NCh sheets were ground before testing. The 2θ degree was set to 5-80° and scan rate was 5° per minute.

Fourier transform infrared (FT-IR) and X-ray photon spectroscopies

Infrared spectra were acquired using a Bruker VERTEX 80V FT-IR spectrometer. KBr tablets were used for this purpose. The spectral range was set to 400-4000 cm^{-1}. XPS measurements were carried out in a Shimadzu AXIS UltraDLD using a monochromatic Al KR X-ray source.

Thermogravimetric analysis (TGA)

TGA data (under N_2) were measured with a TA Instruments SDT Q600 thermogravimetric analyzer. The temperature was set from room temperature to 800°C, heating rate was 10 °C/min. HA concentration in LH was calculated from TG by the following equation:

$$HA\% = \frac{\frac{M_{S450}}{M_{S250}} - \frac{M_{C450}}{M_{C250}}}{\frac{M_{S450}}{M_{S250}}}$$

where M_{S250} and M_{S450} correspond to the residual mass of freeze-dried LH at 250 and 450 °C, respectively. M_{C250} and M_{C450} are the residual mass of pure NCh measured at 250 and 450, respectively. The HA content in LH-0.25, LH-0.5 and LH-1 was 40%, 51.5% and 60.61%, respectively.

Scanning electron microscopy (SEM) and Energy Dispersive Spectroscopy (EDS)

SEM images were taken with a JEOL JSM 7600F field emission scanning electron microscope (2-5 kV, depending on the sample state). In order to protect their structures, all samples except the monolithic abiotic calcite and aragonite were observed directly, without gold sputtering. The other samples were gold sputtered for 90 seconds at a constant current of 30 mA before observation. The EDS data were acquired from SEM imaging using an Oxford PentaFET Precision detector.

Three-point bending tests

Three-point bending tests were performed on a Shimazu universal testing machine. For this purpose, the materials were carefully shaped into sheets of 20 mm (length), 5 mm (width) and 0.5 mm (thickness), as well as the natural nacres samples. The loading rate was 1 mm/min. Each sample was repeated for 5 times.

Nanoindentation (NI)

Nanoindentation tests were carried out by using an iMicro nano indenter equipped with a continuous stiffness measurement (CSM) module. The samples were stored and the data were obtained at a relative humidity (RH) of 35% and 25 °C. LP were indented on the fracture surface (parallel to their layers). The indented depth for all samples was 200 nm. The surface stress distribution was also accessed with the nano-indenter. Areas of 20*40 μm were measured and the point was set as 30*150. Before testing, the samples were embedded in resin and the fracture surface was carefully prepared with a diamond cutter to obtain a smooth surface.

Supporting Figures

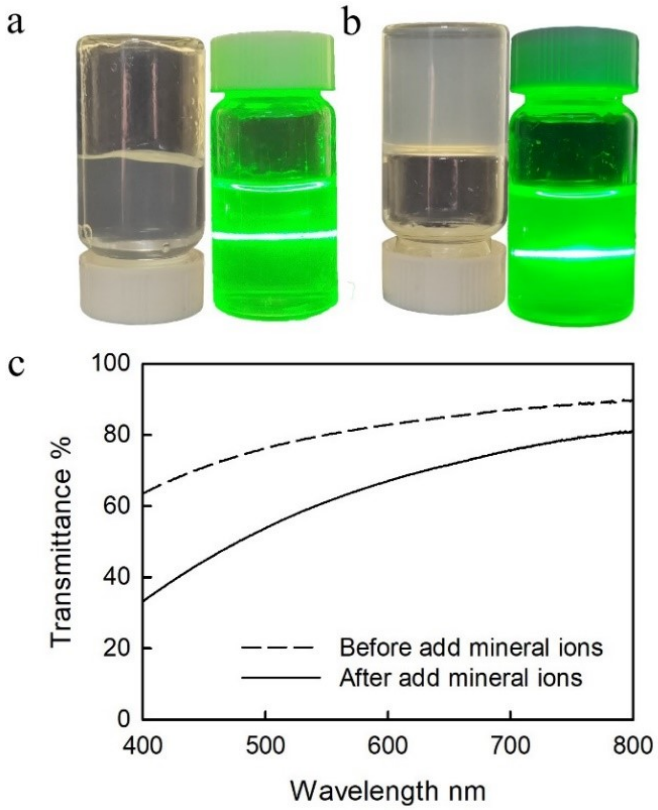

Figure S1. Photograph and transmittance of NCh dispersions. Chitin nanofiber dispersion, 0.5% wt/wt concentration before (a) and after (b) addition of buffer with mineral ion precursor. (c) Light transmittance of the same systems. After adding mineral ion precursor, the transmittance of the dispersion decreased due to ionic cross-linking between calcium and NCh. Following such effect, the fluidity of the aqueous dispersion was significantly decreased.

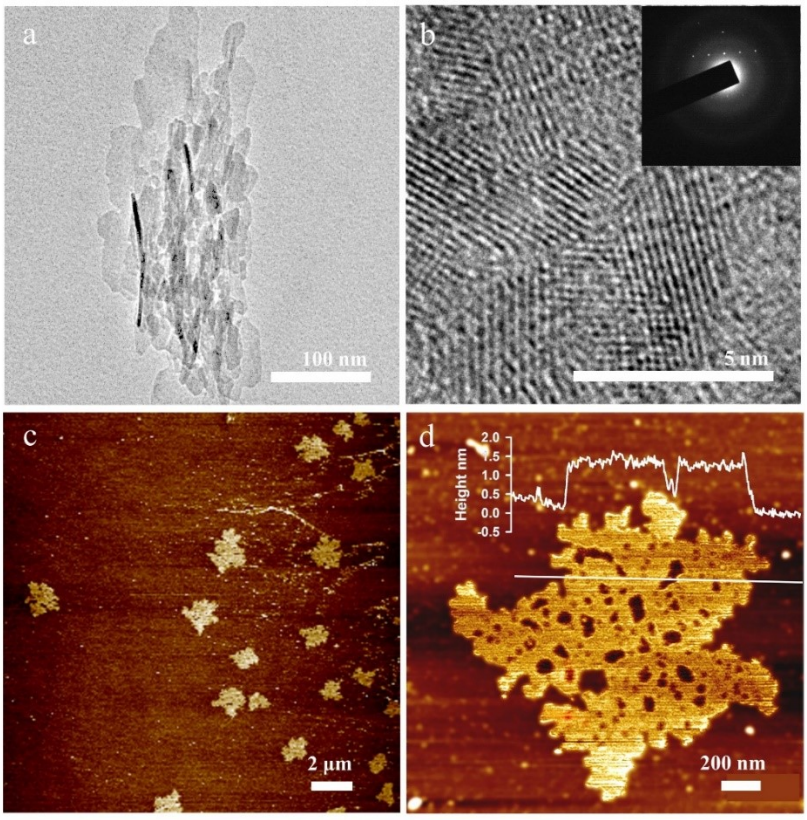

Figure S2. Morphology of HA synthesized in HA-NCh. High Resolution Transmission Electron Microscope (HRTEM) image (a) and Selected Area Electron Diffraction (SAED) of HA nanospheres (b). (c, d) AFM image of HA nanosheet isolated from LH.

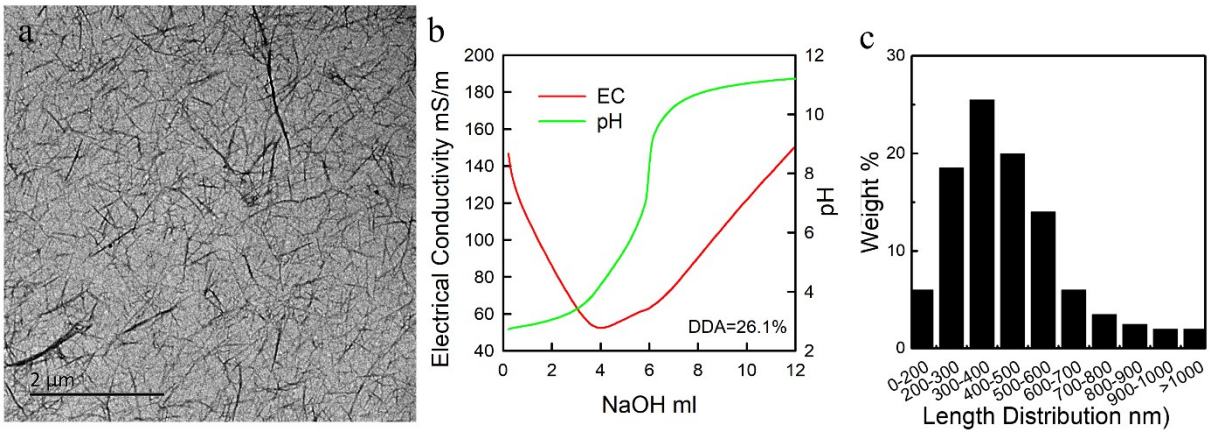

Figure S3. Nanochitin. (a) TEM image of NCh, (b) titration profile and (c) size distribution of the partially deacetylated chitin used in our experiments (NaOH used in titration was 0.05 mmol/L). The degree of deacetylation, DDA, was calculated to be 26.1%.

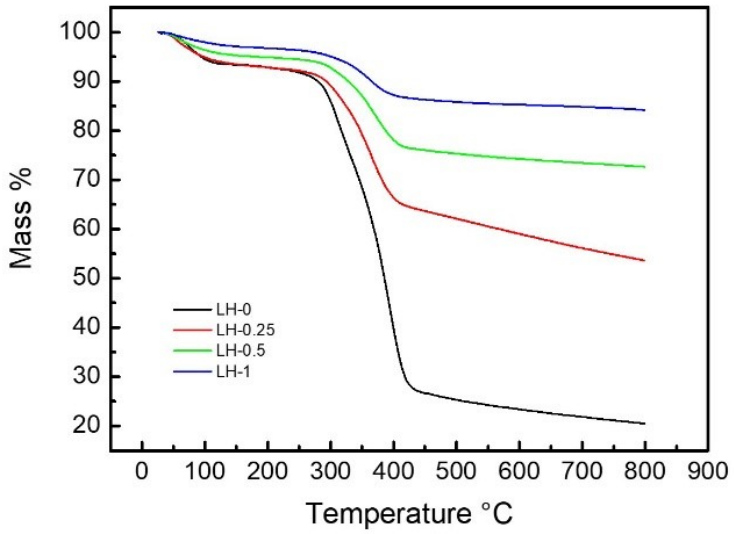

Figure S4. TGA profile of LH under different mineralization conditions. As the concentration of Ca ion increased, the inorganic content of the synthetic HA- NCh increased correspondingly.

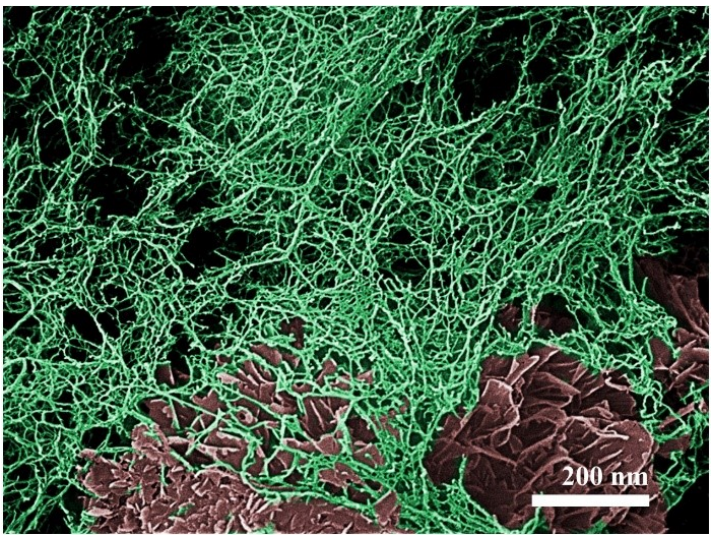

Figure S5. SEM image of HA microsphere embedded in the NCh network. The green network corresponds to NCh around HA nanosheets (indicted in red color).

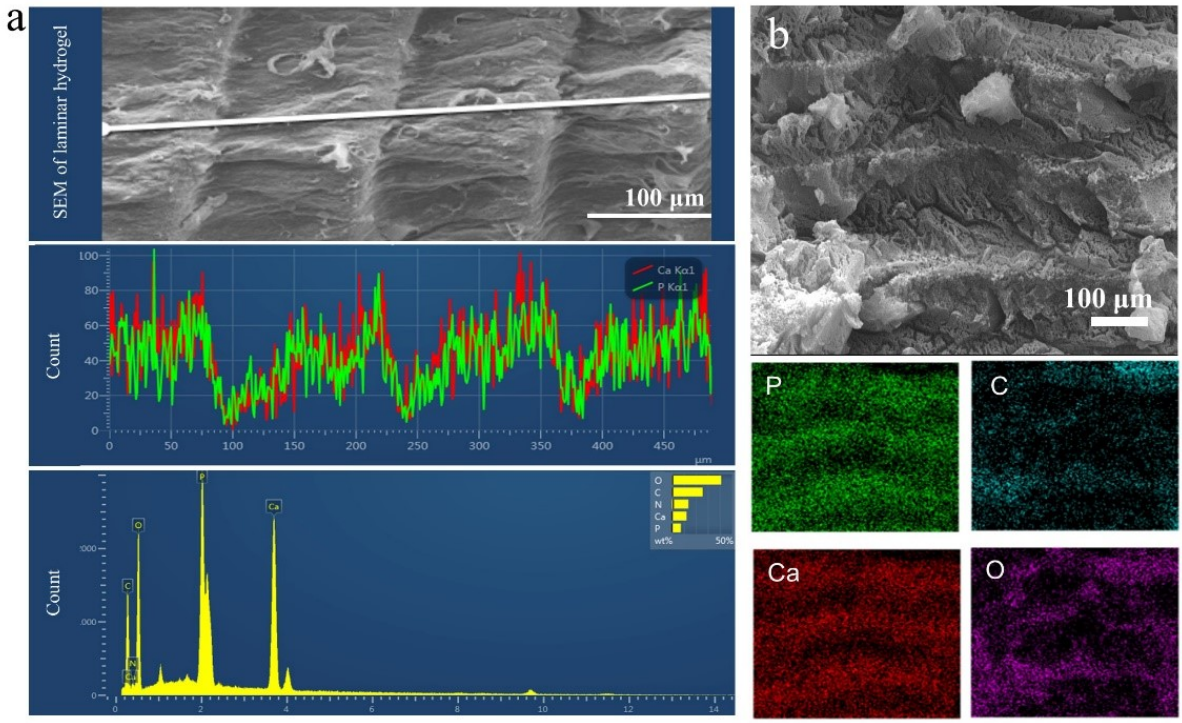

Figure S6. Surface elemental distribution in LH. Ca and P were mainly distributed in the mineralized layers.

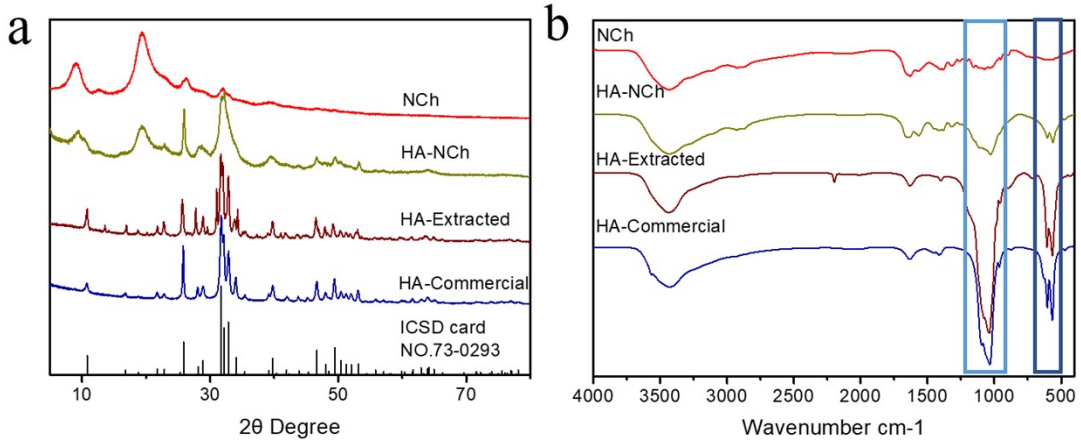

Figure S7. Structural and chemical analysis of HA-NCh. XRD (a) and FTIR (b) patterns of NCh, HA-NCh, HA extracted from HA-NCh using a muffle furnace at 550 °C, and commercial HA obtained from Sinopharm Co. Ltd. PDF card of HA is referenced in the ICSD database. Compared with the PDF card and the commercial HA powder, the mineral synthesized in our work consisted mainly of HA, and small amounts of tricalcium phosphate (β-TCP).

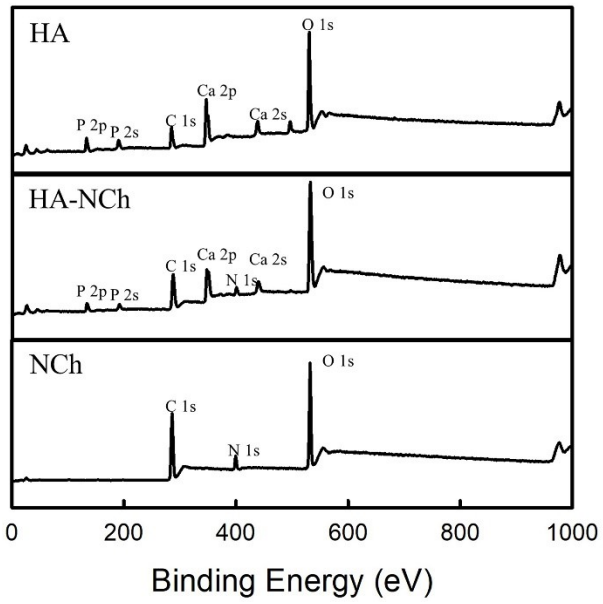

Figure S8. Typical XPS wide scan of NCh. HA-NCh and HA extracted from HA-NCh after removal of the organic phase by using a muffle furnace at 550 °C. Carbon and nitrogen come from NCh, while phosphorus and calcium come from HA

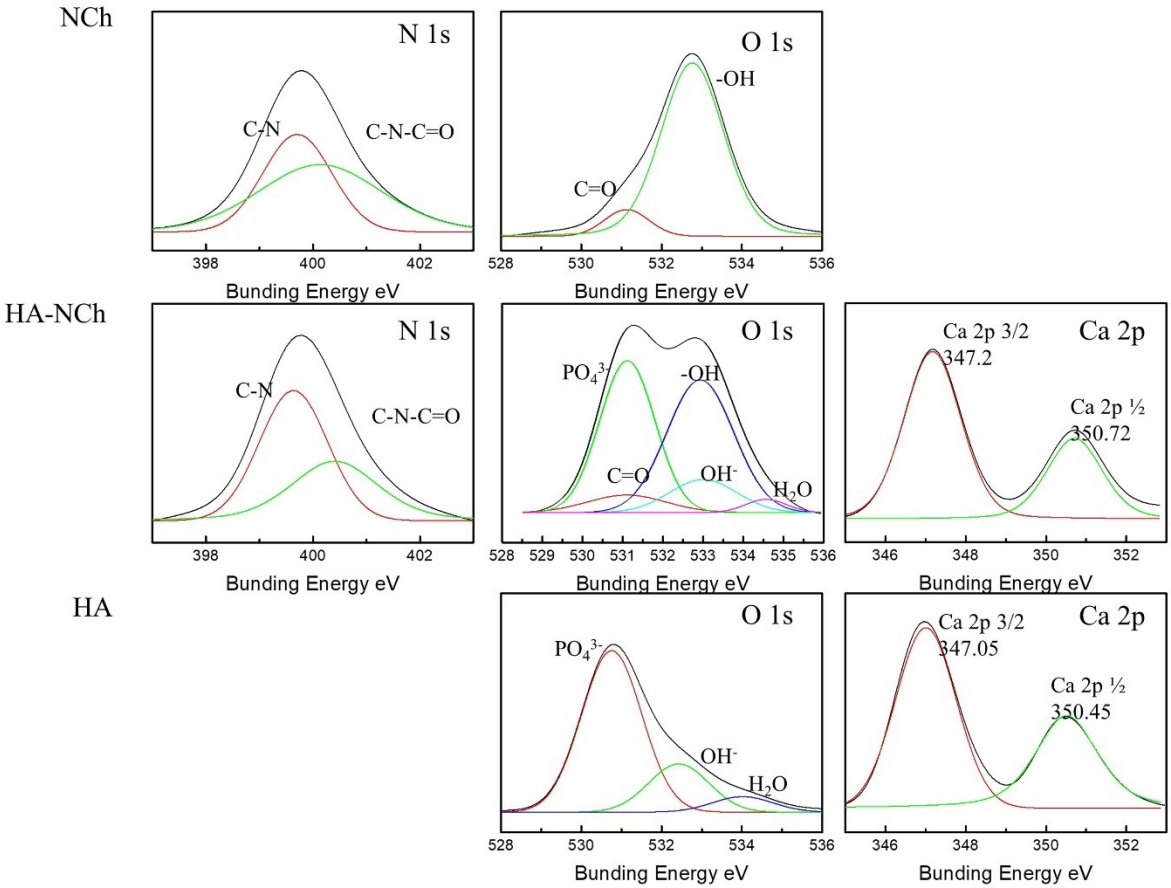

Figure S9. XPS core peaks N 1s, O 1s and Ca 2p of NCh, HA-NCh and HA. Ca was present in HA and N was in NCh while O existed in the two components. The N 1s core peak shows no significant change but the Ca 2p core peak in HA shows a higher binding energy, indicating that HA may interact with NCh.

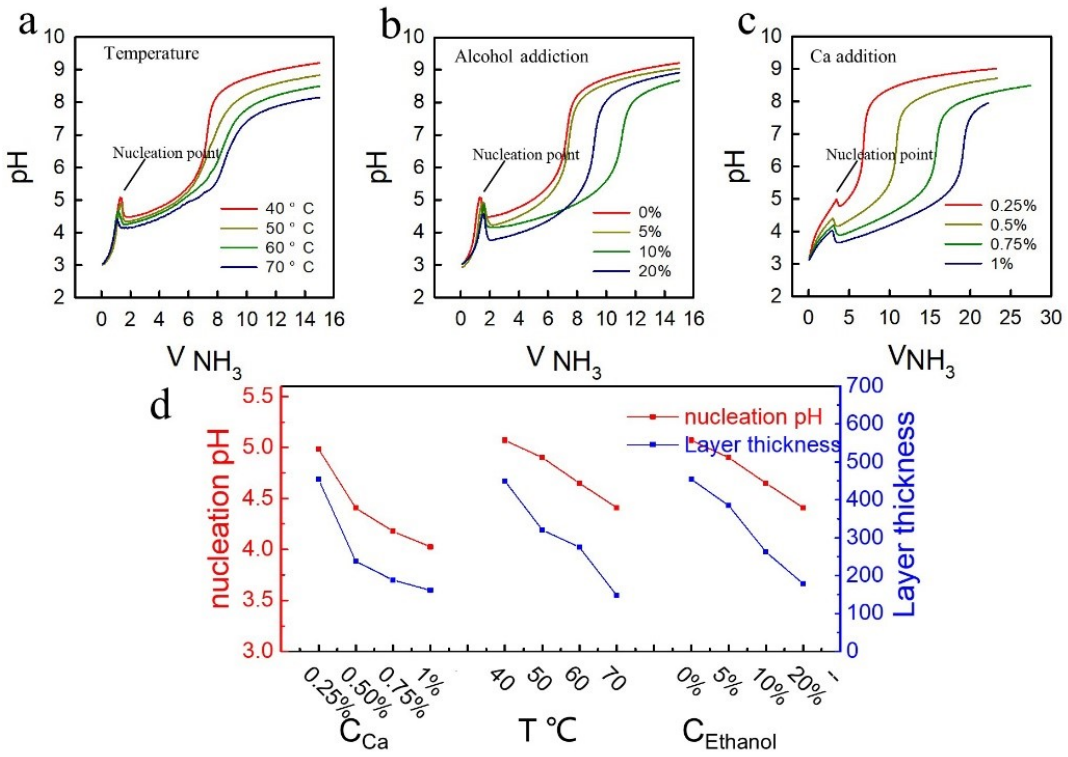

Figure S10. The connection between nuclei pH (threshold pH) and layer spacing. (a-c) Titration diagram of ion precursor solution under different conditions with 5% wt/wt $NH_3 \cdot H_2O$ solution. (d) Relation between nucleation pH and layer thickness for the different conditions tested. The titration diagram shows the changes in nucleation pH of HA, under different conditions. High temperature, addition of ethanol and increase of Ca concentration reduce the nucleation pH, which is linearly related to layer spacing. The layer thickness was the average value of the first 10 mm of mineralized stratification area.

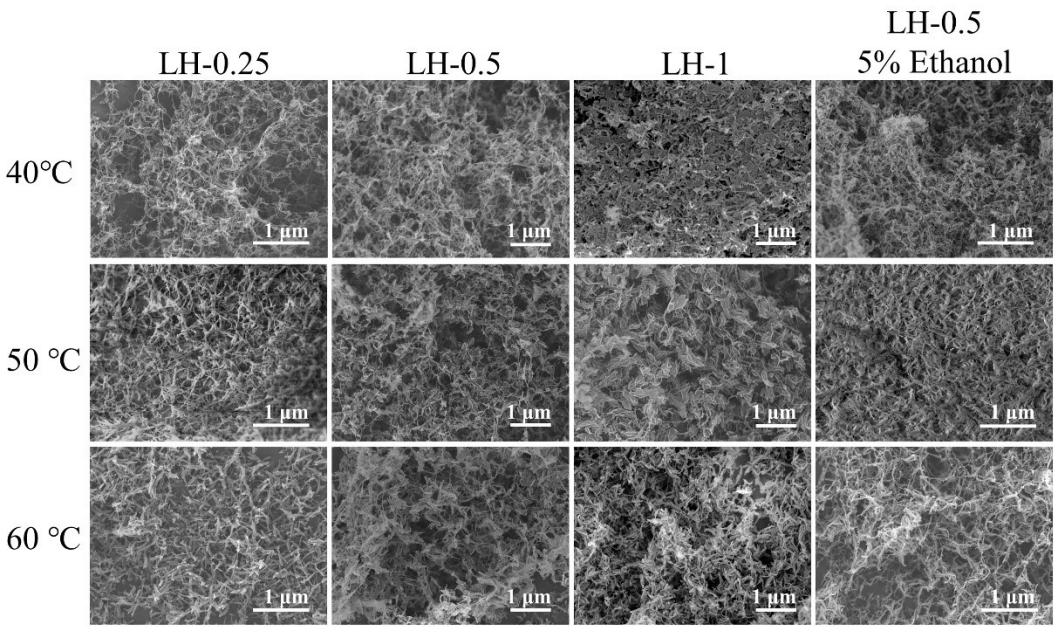

Figure S11. Morphology (SEM) of HA in a uniform layer obtained following the given conditions. HA was uniformly distributed in the NCh uniform layer.

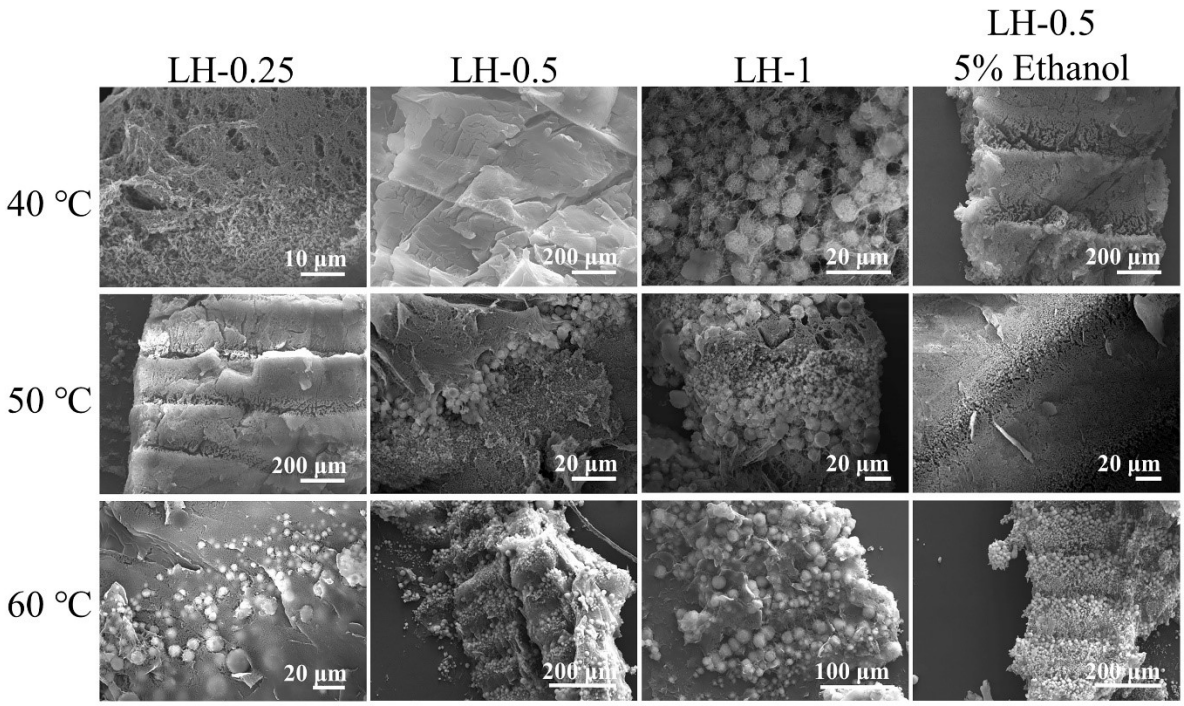

Figure S12. Morphology (SEM) of the lamellar structure obtained under the given conditions. The mineralized layer composed of HA spheres and non-mineralized layers were alternately stacked, forming a periodic structure. High reaction temperature increases the rate of molecular motion and reduces the critical pH of nucleation, promoting the growth of minerals. A high mineral ion concentration will reduce the critical pH, and will have provide ions supporting HA growth and finally leading to bigger HA sphere size.

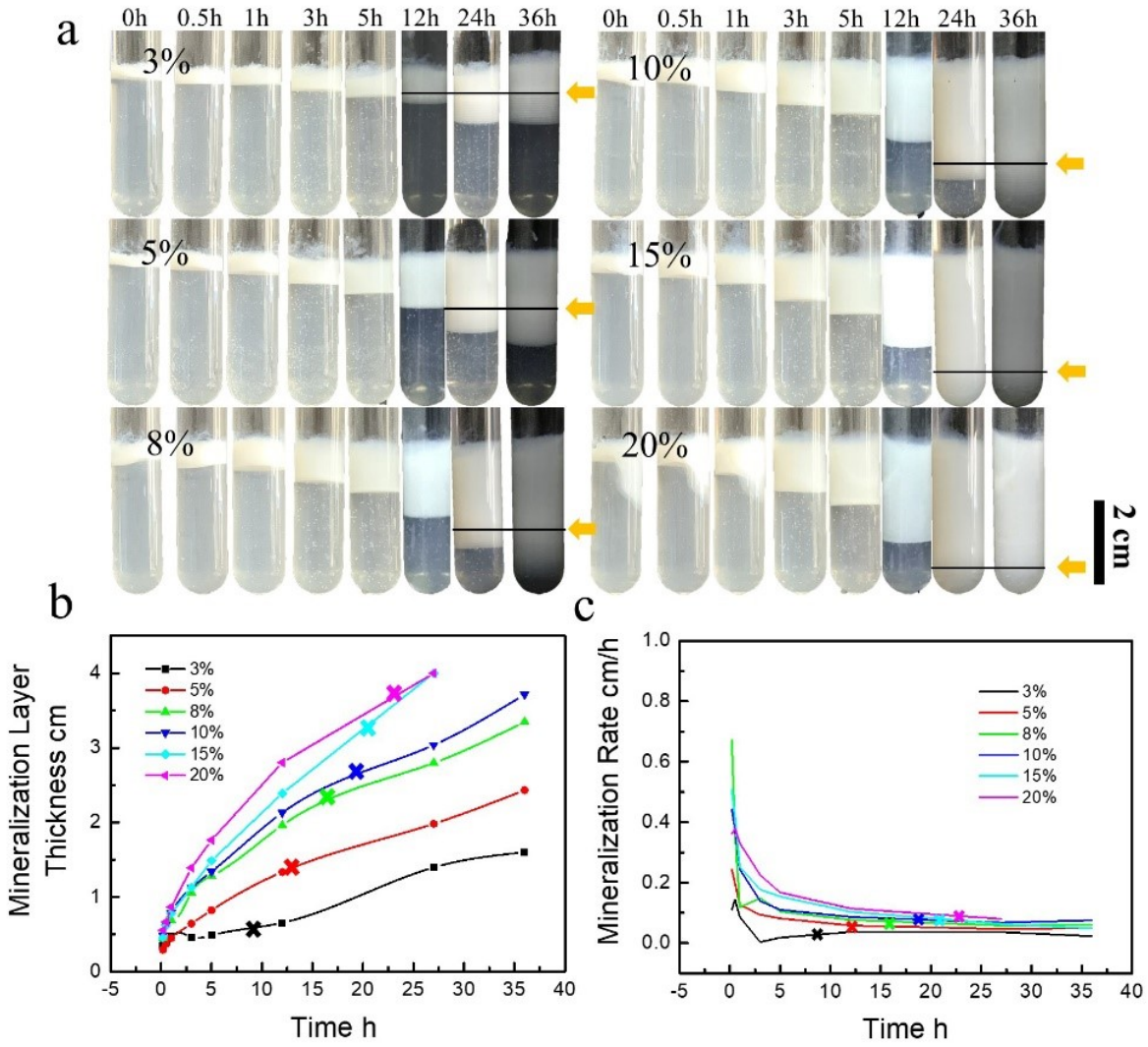

Figure S13. Use of ammonia solution in the preparation of HA-NCh hydrogels. (a) Digital photos of the mineralization processes as a function of time for different concentration of ammonia solution. (b) Corresponding mineralization layer thickness and (c) mineralization rate. Different concentration of ammonia solutions were directly placed at the top of the dispersion mixture. The mineralization process was continued for 36 h, the black lines and yellows arrows show the onset of stratification position and the data can be seen in graph b and c. The mineralization rate was very high and decreased with time. The higher the initial ammonia concentration, the faster the diffusion rate of the sample, but the later the mineralization stratification occur (NCh 0.5%, Ca 0.5%, T 30 °C).

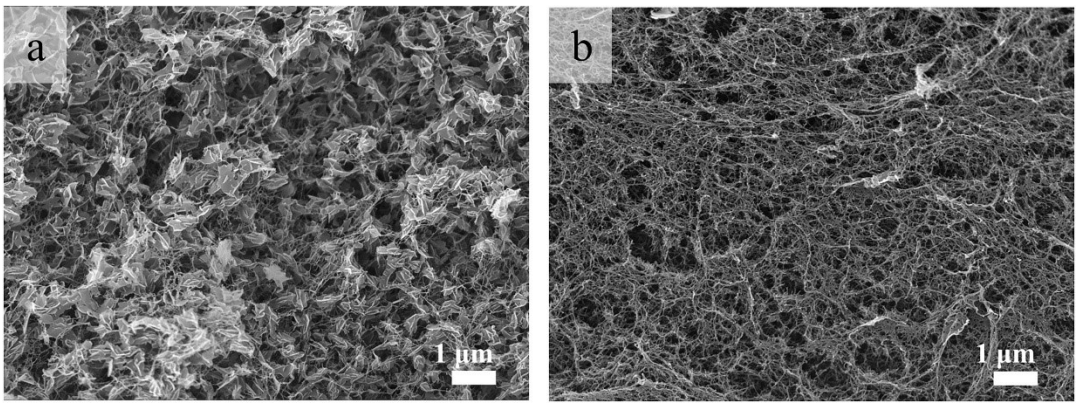

Figure S14. SEM image of the cross-section of LH. (a) mineralized layer, (b) nonmineralized layer. The HA spheres observed in the cross-section image of the mineralized layer displayed similar sizes, while no spheres where apparent in the non-mineralization layer (NCh 0.5%, Ca 0.5% , T 45°C).

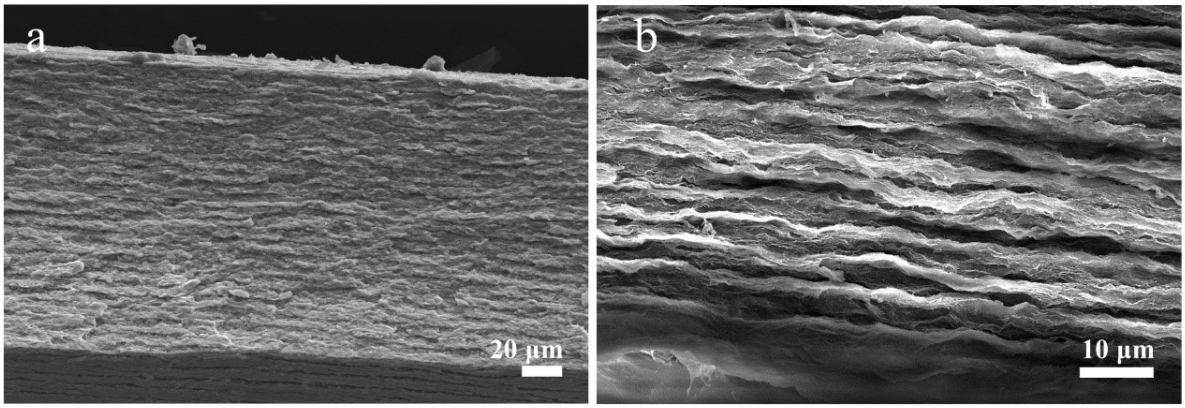

Figure S15. SEM image of the fracture surface of mineralized and demineralized samples. (a) Fracture view of the synthetic nacre showing the multilayer fracture edge. (b) The lamellar chitin layer is seen after removal of HA. The sample was immersed in 1 M HCl for several hours to remove HA.

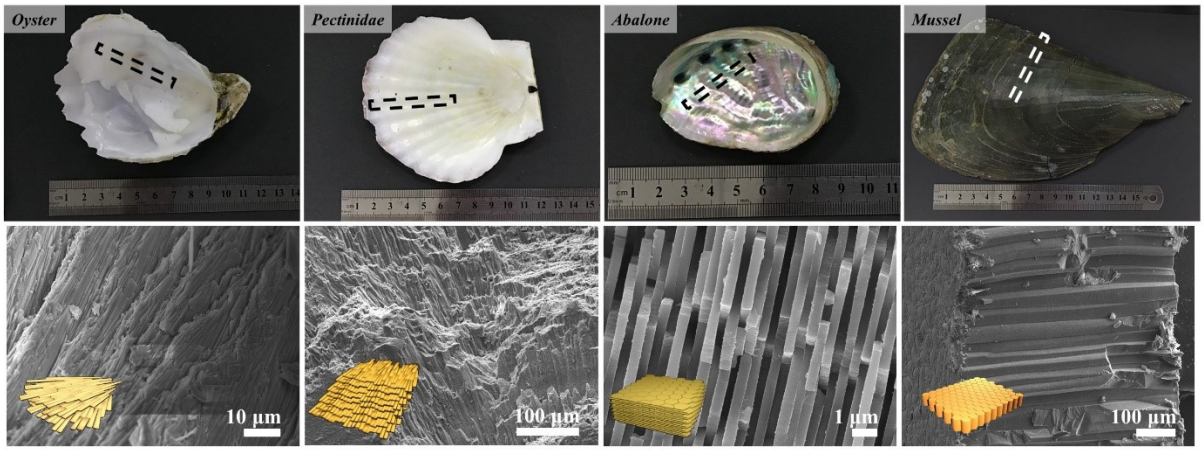

Figure S16. Digital photos and SEM images of natural nacres. The areas marked with the dotted lines were used to test the mechanical strength.

Supporting Movies

Movie S1. Animation to illustrate the formation process of HA-NCh hydrogels following layered mineralization (the movie was made by using 3Dmax).

Movie S2. The process of formation of HA-NCh hydrogels with layered mineralized structure by IDGG. pH indicator (methyl red – bromocresol green) was added in the left container, the color change range corresponded to pH 5.0 - 5.2. The container on the right shows the normal mineralization process, without pH indicator. About 24 h were needed to complete this mineralization and gelation process (Ca 0.2% wt/wt, NCh 0.4% wt/wt, T 40 °C, Ca:P 1.67).

Movie S3. The selective light transmission of LH (Ca 0.1% wt/wt, NCh 0.4% wt/wt, T 40°C, Ca:P 1.67).